A Linear Magnetic-geared Free-piston Generator for Range-extended Electric Vehicles

Wenlong Li [1] and K. T. Chau [2]

[1] *Department of Electrical and Electronic Engineering, The University of Hong Kong, wlli@eee.hku.hk*
[2] *Department of Electrical and Electronic Engineering, The University of Hong Kong, ktchau@eee.hku.hk*

Abstract

This paper proposes a novel linear magnetic-geared machine for the free-piston generator in range-extended electric vehicles. The key is to integrate a linear magnetic gear into a linear permanent magnet synchronous machine to form a single machine, which can offer high efficiency and high power density for electricity generation. The low-speed mover of the proposed machine is directly coupled with the pistons of the internal combustion engine and reciprocates with the pistons. Due to the magnetic gear effect, the high-speed mover which is also the translator of the synchronous machine can travel at high speeds, hence offering high power density design and generating electricity with a high voltage. By using finite element analysis, the machine performance is analyzed and verified.

Keywords

linear magnetic gear, linear synchronous machine, free-piston generator, range-extended electric vehicle, integrated machine

1. INTRODUCTION

With ever-increasing concerns on global environmental deterioration and fossil energy shortage, there is a fast growing interest in electric vehicles (EVs) for road transportation. EVs can be classified into three main kinds: battery EVs, fuel cell EVs and hybrid EVs (HEVs). Due to the consideration on driving range and initial cost, the HEV which incorporates an internal combustion engine (ICE) and an electric motor has been successfully commercialized by automakers [Chan and Chau, 2001; Chau et al., 1999; Chau et al., 2007; Zhang et al., 2008].

According to the relationship between the ICE, electric motor and transmission system, the HEVs can be classified as the series hybrid, parallel hybrid, series-parallel hybrid and complex hybrid. The series hybrid is the simplest kind of HEVs. Its engine output is first converted into electricity using a generator. The converted electricity either charges a battery set or propels the wheels via an electric motor and mechanical transmission system [Chau and Wong, 2001].

The range-extended electric vehicle (REV) is a new concept of series HEVs. It is designed that the electric motor propels the vehicle whenever possible. When the battery voltage falls below a certain level, it can be plugged into the grid for charging or charged by an onboard generator. In this REV, a rotational generator is adopted to convert the engine power into electricity.

Because of the linear motion of ICE pistons, crankshafts and connecting rods are usually involved for linear-to-rotational motion conversion. The intermediate mechanical system results in low efficiency and low power density. Thus, the free-piston generator (FPG) is a good solution for substitution which integrates an ICE and a linear electrical generator into a single unit [Mikalsen and Roskilly, 2007]. As shown in Figure 1, by directly coupling the ICE to the linear generator, it benefits in efficiency, weight reduction and robustness.
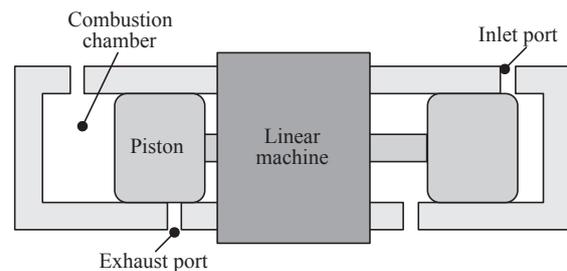

Fig. 1 Free-piston generator

A suitable linear machine topology is vital for the FPG. Over decade years of research, a lot of linear machine configurations were proposed and investigated [Faiz et al., 2006; Zhang et al., 2007; Arshad et al., 2004]. The linear transverse-flux machine (TFM) which has a high force density and high power density was claimed as the most suitable electrical machine for the free-piston generator [Arshad et al., 2002]. However, the TFM generally suffers from a low power factor, a complex configuration and a high manufacturing cost which hinder its practical application.

The purpose of this paper is to propose a novel linear magnetic-geared machine which integrates a linear permanent magnet (PM) synchronous machine with a linear magnetic gear for the free-piston generator. Because of inherent high force density of the linear magnetic gear [Atallah et al., 2005], the power density of the integrated machine can be greatly improved.

2. MACHINE DESIGN

Figure 2 shows the topology of the proposed linear magnetic-geared machine. It integrates a linear magnetic gear into a linear PM synchronous machine to form a single machine by artfully sharing a common moving part, namely the high-speed mover of the linear magnetic gear and the translator of the linear PM synchronous machine. It has a tubular structure with four main parts: the low-speed mover, the stationary modulation rings, the high-speed mover (which is also the translator) and the stator. The low-speed mover is an iron yoke with longitudinal-magnetized PMs

mounted on its surface. The high-speed mover is an iron yoke sandwiched by two rows of PMs. The modulation rings lie between the low-speed mover and the high-speed mover, which are made of steel and mechanically fixed with epoxy. The stator is installed with 3-phase AC windings for electricity generation. In order to minimize the cogging force which is one of the major problems in linear PM machines, the total stator length is specially adjusted [Li and Chau, 2010]. The key design data are listed in Table 1.

The operation principle is that the low-speed mover reciprocates with the pistons. Then, by the magnetic gear effect, the speed of the high-speed mover is amplified accordingly. The force transmission between the low-speed mover and high-speed mover is based on the modulation of air-gap flux density distribution along the longitudinal direction. Like its rotational counterpart, the linear magnetic gear is governed by the following equations [Chau et al., 2007; Chau et al., 2008; Jian et al., 2009; Jian and Chau, 2009]:
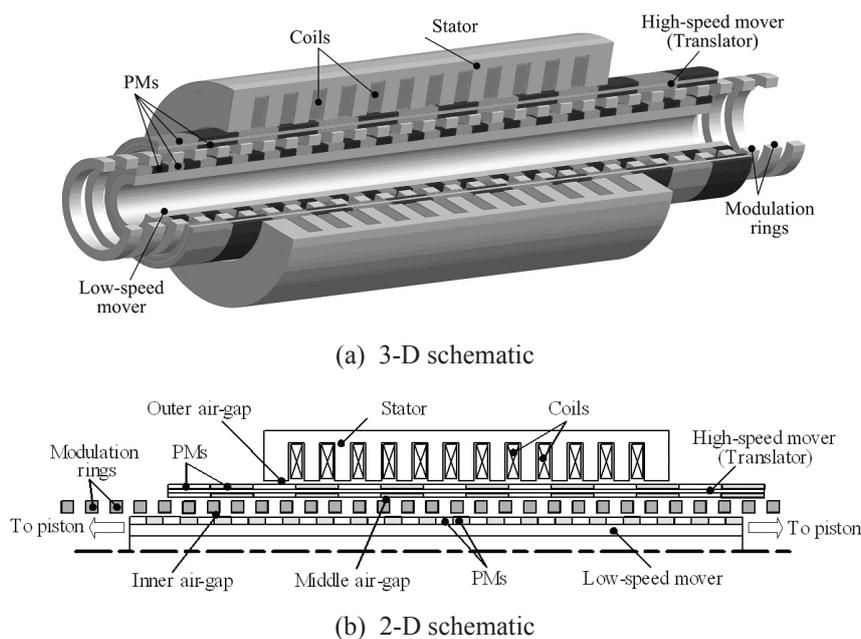
$$n_s = p_{lm} + p_{hm} \tag{1}$$

$$G_r = -\frac{p_{lm}}{p_{hm}} \tag{2}$$

$$G_r = \frac{v_{hm}}{v_{lm}} \tag{3}$$

$$G_r = -\frac{F_{lm}}{F_{hm}} \tag{4}$$

where p_{lm} is the number of active PM pole-pairs on the low-speed mover, p_{hm} is the number of active PM pole-pairs on the high-speed mover, n_s is the number

Table 1 Key design data

Rated power	10 kW
Rated voltage	220 V
Inside radius of low-speed mover	12 mm
Outside radius of low-speed mover	22 mm
Inside radius of modulation rings	23 mm
Outside radius of modulation rings	29 mm
Inside radius of high-speed mover	30 mm
Outside radius of high-speed mover	37 mm
Inside radius of stator	38 mm
Outside radius of stator	64 mm
Active length	264 mm

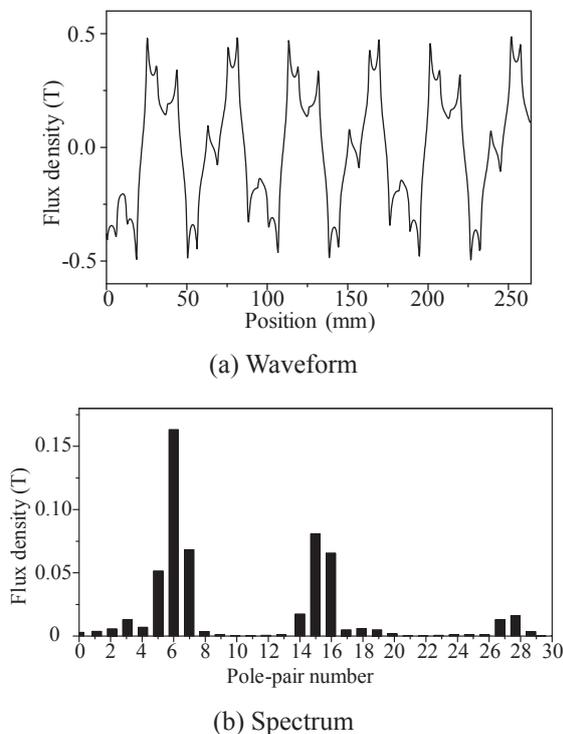(a) 3-D schematic

(b) 2-D schematic

Fig. 2 Proposed linear magnetic-geared machine

of active stationary modulating ring pole-pieces, G_r is the gear ratio, v_{hm} is the speed of high-speed mover, vlm is the speed of low-speed mover, F_{hm} is the thrust force of high-speed mover, F_{lm} is the thrust force of low-speed mover, and the minus sign denotes that the two movers travel in opposite direction but the thrust force directions of the two movers are in the same direction. In this design, p_{lm} is 15, p_{hm} is 6, and n_s is 21. Hence, $G_r = -2.5$ is resulted.
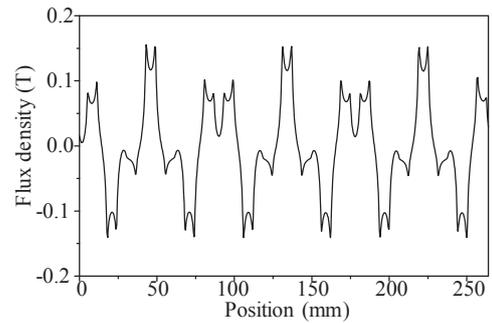
3. MACHINE ANALYSIS

The proposed machine has a tubular structure which means that the leakage flux due to the transverse finite length is much smaller than that of the flat one. Thus, the 2-D time-stepping finite element method (TS-FEM) is adopted for analysis.
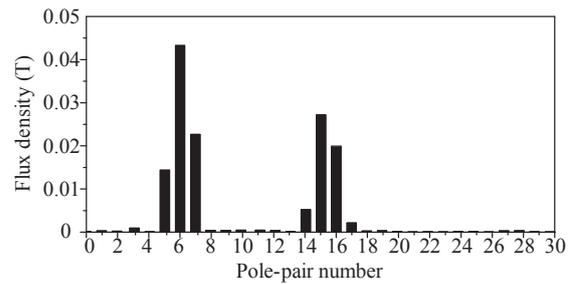
Figure 3 shows the inner air-gap longitudinal flux density waveform and its spectrum when only the PMs on the high-speed mover are considered as excitation sources and the PMs on the low-speed mover are considered as air. Due to the field modulation rings, the largest asynchronous harmonic component (namely the pole-pair number of 15) which interacts with the 15 pole-pair PMs on the low-speed mover to develop a thrust force. Similarly, Figure 4 shows the middle air-gap longitudinal flux density waveform and its spectrum due to PMs on the low-speed mover. It can be observed that the largest asynchronous harmonic component is the pole-pair number of 6, which inter-
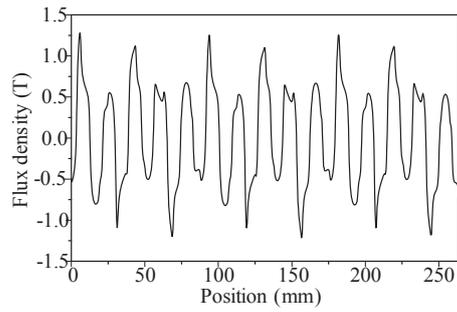

(a) Waveform

(b) Spectrum

Fig. 4 Middle air-gap longitudinal flux density due to PMs on low-speed mover
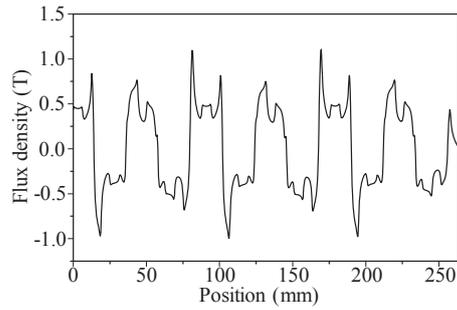
acts with the 6 pole-pair PMs on the high-speed mover to develop a thrust force.

When all PMs are taken into account, the flux density waveforms in three air-gaps are depicted in Figure 5. With the detailed knowledge of field distribution, the developed force of the movers can be determined by Maxwell tensor. When the high-speed mover is fixed and the low-speed mover travels a pole-pitch, the static thrust characteristic can be obtained as shown in Figure 6. The thrust force of the low-speed mover is about 2.5 times that of the high-speed mover thrust force. The peak thrust force of the low-speed mover is 2.6 kN.
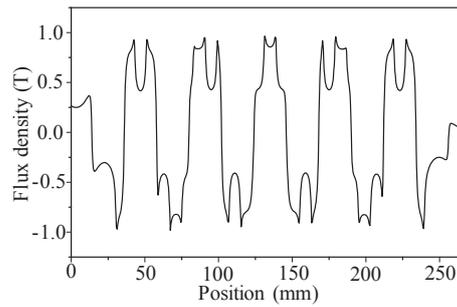
When the low-speed mover travels at 5 m/s, and the high-speed mover travels at 12.5 m/s with an opposite direction, the force transmission capacity of the linear magnetic gear can be obtained. Figure 7 shows the force transmission waveform in which the force of the low-speed mover keeps at about 2 kN, and the force of the high-speed mover is about 900 N. It can be found that the force ripple of the high-speed mover is slightly higher than that of the low-speed mover. It is due to the fact that the cogging force of the high-speed mover is the sum of the cogging force of the linear magnetic gear and the cogging force of the linear PM synchronous machine. The resulting induced voltage waveform of the machine is shown in Figure 8 at which the high-speed mover travels at a constant speed of 12.5 m/s.

(a) Waveform

(b) Spectrum

Fig. 3 Inner air-gap longitudinal flux density due to PMs on high-speed mover

(a) Inner air-gap

(b) Middle air-gap

(c) Outer air-gap

Fig. 5 Flux density waveforms in three air-gaps
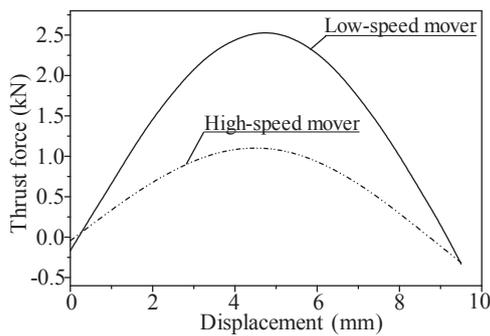
Fig. 6 Static thrust waveform

Fig. 7 Force transmission capacity

Fig. 8 Induced voltage waveform

cm^3, 7.4 g/cm^3 and 9.0 g/cm^3 respectively, the total weight is 18.95 kg. Thus, the specific power of the proposed machine is 0.53 kW/kg.

5. CONCLUSION

By integrating a linear magnetic gear into a linear synchronous machine, the resulting linear magnetic-geared machine can offer high power density. With the help of linear magnetic gear, the whole system is downsized, and the translator speed of the synchronous machine is amplified. Thus, the desired voltage level can be generated by using only a small number of turns of windings. Therefore, the proposed generator is very promising to work for the free-piston generator in REVs.

Acknowledgements

References

Arshad, W. M., P. Thelin, T. Backstrom, and C. Sadarangani, Use of transverse-flux machines in a free-piston generator, *IEEE Transactions on Industry Applications*, Vol. 40, No. 4, 1092-1100, 2004.

Arshad, W. M., T. Backstrom, P. Thelin, and C. Sadarangani, Finding an appropriate electrical machine for a free piston generator, *Proceeding of*

4. DISCUSSION

With the aid of high force density linear magnetic gear, the total size of the proposed machine is reduced. The corresponding iron material is 1655 cm^3, PM material is 483 cm^3 and copper material is 312 cm^3. Since the mass densities of iron, PM and copper are 7.6 g/
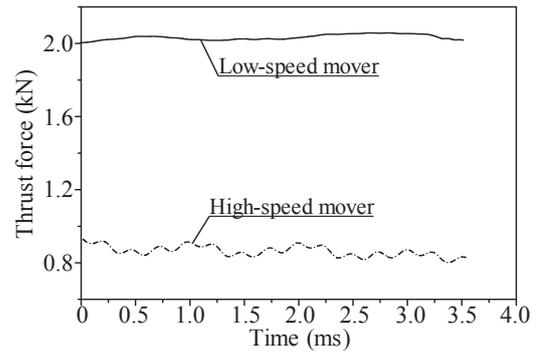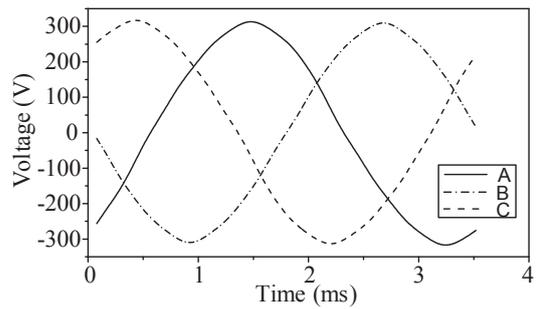
International Battery, Hybrid and Fuelcell Electric Vehicle Symposium and Exhibition, 2002.

Atallah, K., J. Wang, and D. Howe, A high-performance linear magnetic gear, *Journal of Applied Physics*, Vol. 97, No. 10, 10N516:1-3, 2005.

Chan, C. C., and K. T. Chau, *Modern Electric Vehicle Technology*, Oxford University Press, 2001.

Chau, K. T., and C. C. Chan, Emerging energy-efficient technologies for hybrid electric vehicles, *Proceedings of IEEE*, Vol. 95, No. 4, 821-835, 2007.

Chau, K. T., and Y. S. Wong, Hybridization of energy sources in electric vehicles, *Energy Conversion and Management*, Vol. 42, No. 9, 1059-1069, 2001.

Chau, K. T., D. Zhang, J. Z. Jiang, and L. Jian, Transient analysis of coaxial magnetic gears using finite element comodeling, *Journal of Applied Physics*, Vol. 103, No. 7, 07F101:1-3, 2008.

Chau, K. T., D. Zhang, J. Z. Jiang, C. Liu, and Y. J. Zhang, Design of a magnetic-geared outer-rotor permanent-magnet brushless motor for electric vehicles, *IEEE Transactions on Magnetics*, Vol. 43, No. 6, 2504-2506, 2007.

Chau, K. T., Y. S. Wong and C. C. Chan, An overview of energy sources for electric vehicles, *Energy Conversion and Management*, Vol. 40, No. 10, 1021-1039, 1999.

Faiz, J., B. Rezaeealam, and S. Yamada, Reciprocating flux-concentrated induction generator for free-piston generator, *IEEE Transactions on Magnetics*, Vol. 42, No. 9, 2172-2178, 2006.

Jian, L., and K. T. Chau, Design and analysis of an integrated Halbach-magnetic-geared permanent-magnet motor for electric vehicles, *Journal of Asian Electric Vehicles*, Vol. 7, No. 1, 1213-1219, 2009.

Jian, L., K. T. Chau, and J. Z. Jiang, A magnetic-geared outer-rotor permanent- magnet brushless machine for wind power generation, *IEEE Transactions on Industry Applications*, Vol. 45, No. 3, 954-962, 2009.

Li, W., and K. T. Chau, Design and analysis of a novel linear transverse flux permanent magnet motor using HTS magnetic shielding, *IEEE Transactions on Applied Superconductivity*, 2010 (In press).

Mikalsen, R., and A. P. Roskilly, A review of free-piston engine history and applications, *Applied Thermal Engineering*, Vol. 27, No. 14-15, 2339-2352, 2007.

Zhang, P., A. Chen, P. Thelin, W. M. Arshad, and C. Sadarangani, Research on tubular longitudinal flux PM linear generator used for free-piston energy converter, *IEEE Transactions on Magnetics*, Vol. 43, No. 1, 447-449, 2007.

Zhang, X., K. T. Chau, and C. C. Chan, Overview of thermoelectric generation for hybrid vehicles, *Journal of Asian Electric Vehicles*, Vol. 6, No. 2, 1119-1124, 2008.